

## Phase Composition and Defect Substructure of Double Surfacing, Formed with V–Cr–Nb–W Powder Wire on Steel

S. V. Konovalov<sup>a, \*</sup>, V. E. Kormyshev<sup>a, \*\*</sup>, V. E. Gromov<sup>a</sup>, Yu. F. Ivanov<sup>b, \*\*\*</sup>, and E. V. Kapralov<sup>a</sup>

<sup>a</sup>*Siberian State Industrial University, Novokuznetsk, 654007 Russia*

<sup>b</sup>*Institute of High Current Electronics, Siberian Branch, Russian Academy of Sciences, Tomsk, 634021 Russia*

\**e-mail: konovalov@physics.sibsiu.ru*

\*\**e-mail: gromov@physics.sibsiu.ru*

\*\*\**e-mail: yufi55@mail.ru*

Received February 17, 2016

**Abstract**—The analysis of phase composition, defect substructure, and mechanical and tribological properties of Hardox 450 steel after single and double surfacing of C–V–Cr–Nb–W containing wire was carried out by methods of modern physical materials science. The increase in the wear resistance of the material compared to the original steel by 140–150 times and reduction of the friction coefficient by 2–2.5 times was established. The change in the fine structure and phase composition of the surfaced metal was analyzed. It was shown that the established effects could be associated with the formation of a multiphase nanoscale and submicron structure, hardening of which was associated with the formation of martensitic structure of  $\alpha$ -matrix and the presence of a high volume fraction of carbide phase inclusions based on Fe, Cr, W and Nb. Formation of resurfacing led to repeated increase in the volume fraction of the carbide phase and the absence of the oxide phase.

**Keywords:** steel Hardox 450, cladding, structure, phase composition, abrasion resistance, friction coefficient, microhardness

**DOI:** 10.1134/S2075113317020101

### INTRODUCTION

One way to increase the service life of machines and mechanisms, details of which are subjected to abrasion and impact loads during operation, is to apply a coating to them by various methods containing wear-resistant elements [1]. This leads to a substantial increase in the service life of the whole product. Specifically, experimental application of coatings by welding methods, hardened by particles of carbides, borides, and other very hard phases on the buckets of excavators and bodies of dump trucks leads to prolongation of the interval between repairs by almost 1.5 times [2, 3].

Earlier in our papers [3–5], patterns of change in structural-phase states and tribological properties of steel Hardox 400 were established when wear-resistant coatings were applied to them, according to the composition corresponding to medium- and high-alloy steels and high-chromium cast irons. It is shown that cladding is a multiphase material and is represented by the grains of solid solution based on  $\alpha$ -iron and submicro- and nanosized particles of carbide and boride phases—carbides of iron ( $\text{Fe}_3\text{C}$ ), niobium ( $\text{NbC}$ ), and chromium ( $\text{Cr}_3\text{C}_2$ ,  $\text{Cr}_7\text{C}_3$ ), iron borides ( $\text{FeB}$ ,  $\text{Fe}_3\text{B}$ ), iron borosilicides ( $\text{B}(\text{Fe}, \text{Si})_3$ ), and chromium carboborides ( $\text{Cr}_7\text{BC}_4$ ). More than twofold increase in the

wear resistance of the pad weld with respect to the steel volume is revealed, which is caused by the formation of submicro- and nanoscale structures of crystallization of the  $\alpha$ -phase and release of a large volume of high-strength particles of the carbide and boride phases. However, as indicated by previously conducted studies, it is possible to achieve large indicators to improve wear-resistant properties of steel products, particularly upon performing not only single but also double cladding.

Steel of Hardox 450 grade is intended for use under conditions where special requirements are imposed on wear resistance in combination with good properties of cold bending and weldability. Scope of Hardox 450 application: bodies of dump trucks, containers, crushers, screeners, loading devices, measuring hoppers, skip winders, edges of cutting knife, conveyors, buckets, knives, gears, chain wheels, etc. [6].

The purpose of this work is analysis of the phase composition, defect substructure, and mechanical and tribological properties of steel Hardox 450 after single and double cladding of C–V–Cr–Nb–W-containing wire.

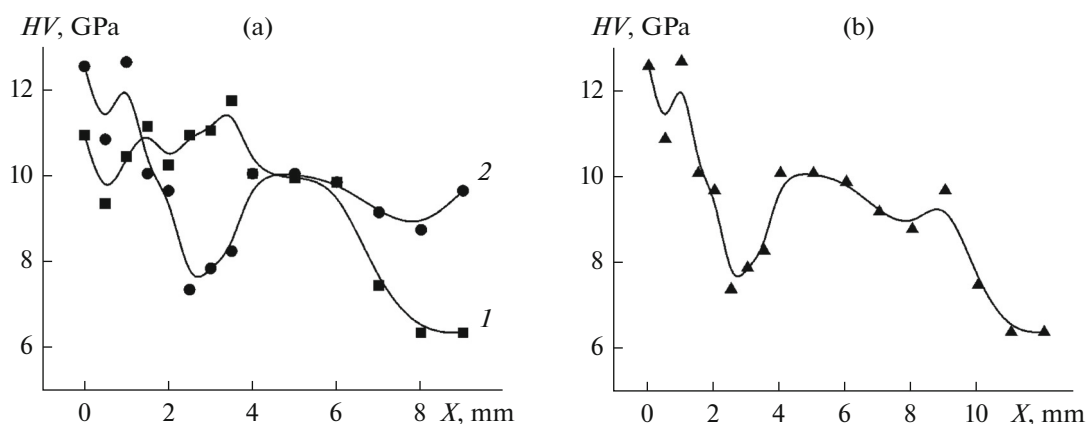


**Fig. 1.** Microhardness profile of the system “weld layer/steel” (a) and “double weld layer” (b); (1) single cladding; (2) double cladding.

## MATERIALS AND METHODS

As a base material, steel of Hardox 450 brand was used. The elemental composition of steel Hardox 450 in wt % is the following: 0.19–0.26 C, 0.70 Si, 1.6 Mn, 0.025 P, 0.010 S, 0.25 Cr, 0.25 Ni, 0.25 Mo, 0.004 B, balance Fe. Double cladding was applied perpendicular to single. Cladding was performed in the medium of protective gas of the composition 82% Ar, 18% CO<sub>2</sub> at welding current of 250–300 A and voltage on the arc of 30–35 V.

Studies of the phase composition and defective substructure of steel and weld metal was carried out by the methods of X-ray analysis (Shimadzu XRD 6000 diffractometer) and transmission electron microscopy (method of thin foils) on a JEM-2100 microscope. Foils were made by electrolytic thinning of the plates, cut from the weld metal (layer located at a half of the thickness of weld metal), contact zones of weld metal and steel, and at the distance of  $\approx 15$  mm from the contact zone in the sample volume of steel. The mechanical properties of weld metal and steel were characterized by microhardness value on an HVS-1000A

microhardness tester (Vickers method, load on the indenter of 5 N). The tribological properties of the weld metal and steel were analyzed by determining the wear resistance and friction coefficient. The volume of wear of the surface layer was determined after performing profilometry of the formed track using a MicroMeasure 3D Station laser optical profilometer.

## RESULTS AND DISCUSSION

Results of the study of microhardness (section, microhardness profile) are presented in Fig. 1. Single cladding leads to the formation of a high-strength surface layer with the thickness of  $\approx 6$  mm, whose microhardness varies in the interval of 9.5–11.5 GPa (Fig. 1, curve 1). With increasing distance from the weld surface, the microhardness of the material decreases rapidly, reaching the level of 6.5 GPa. Consequently, the hardness of the weld layer is almost two times higher than the hardness of the base metal (Hardox-450 steel).

Formation of the second weld layer of the surface layer is accompanied by an increase in the hardness of the surface layer with the thickness of  $\approx 1$  mm to 12.5 GPa and formation of a weakened subsurface layer, located at the depth of 2.5–3.5 mm (Figs. 1a, 1b, curve 2). At greater depth, the hardness of the weld layer increases again to the values of 9.5–10 GPa. It can be assumed that a substantial decrease in the microhardness of the layer located at the depth of 2.5–3.5 mm corresponds to the contact zone of metal of the first and second cladding; repeated increase in the hardness detected at the depth of 4–6 mm is due to the presence of the first weld layer.

The results of tribological tests of steel and metal formed upon single and double claddings are listed in Table 1. The cladding layer located at half of its thickness was subjected to testing.

Analyzing the results presented in Table 1, one can note that the wear resistance of the weld metal exceeds the wear resistance of steel by 140–150 times; the fric-

**Table 1.** The results of tribological tests of steel Hardox 450 and metal layers welded on it

Mode	$V, 10^{-6},$ $\text{mm}^3/(\text{N m})$	$\langle \mu \rangle$	$\mu_{\min}$	$\mu_{\max}$
Steel Hardox 450	95.1	0.259	0.03	0.58
Single cladding	0.69	0.104	0.08	0.14
Double cladding	0.62	0.132	0.11	0.27

$V$ —parameter characterizing the degree of wear of the material;  $\langle \mu \rangle$ —average value of the friction coefficient;  $\mu_{\min}$ —minimum value of the friction coefficient;  $\mu_{\max}$ —maximum value of the friction coefficient.

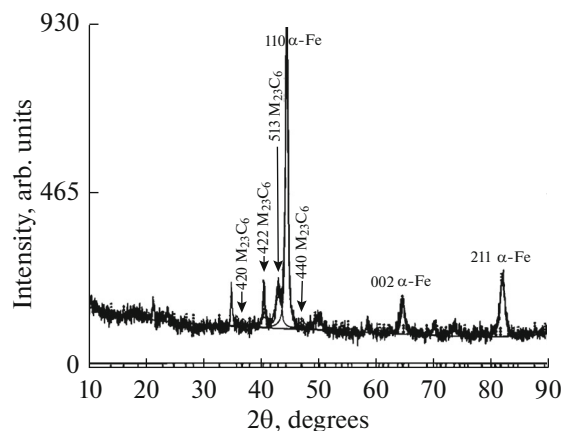


**Fig. 2.** Plot of radiograph obtained from metal sample of repeated cladding.

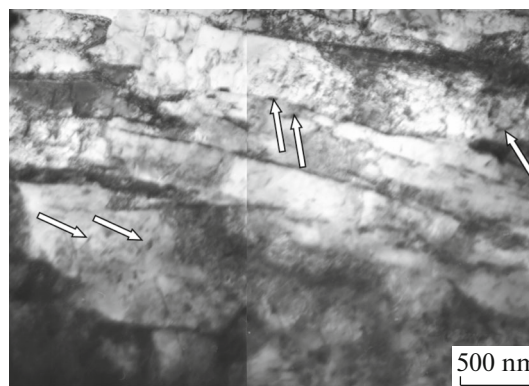


**Fig. 3.** Electron microscopic image of steel structure; arrows indicate the particles of the carbide phase.

tion coefficient of the weld metal is 2–2.5 times lower than the friction coefficient of steel. Formation of the second weld layer has virtually no effect on the tribological characteristics of the material.

It is obvious that increased strength and tribological properties of the metal of cladding are caused by its phase composition and the state of defective substructure. The phase composition of single and repeatedly welded layers was studied by the methods of X-ray analysis. The cladding layer located at half of its thickness was subjected to studies. The X-ray diffraction pattern obtained from the metal sample of repeated welding is shown in Fig. 2. The results of studies of the structure-phase state of the material are presented in Tables 2 and 3.

Analyzing the results presented in Tables 2 and 3, one can note that, in both cases (single and double cladding), a multiphase structure is revealed. The main phase (not including  $\alpha$  phases—solid solution based on BCC of iron crystal lattice) in single cladding is iron oxide of  $\text{Fe}_3\text{O}_4$  composition. The main phase of the repeatedly welded layer is carbides based on special elements (carbides of niobium, tungsten, and chromium). It should also be noted that the formation of repeated cladding leads to multiple increase in the volume fraction of the carbide phase and complete absence of the oxide phase.

The defect substructure of steel and repeatedly welded metal was analyzed by the methods of transmission electron microscopy. Studies showed the structure characteristic of “tempered martensite” [7, 8], i.e., a structure formed as a result of hardening and subsequent tempering of steel (Fig. 3).

Analysis of the images of the steel structure shown in Fig. 3, obtained by the methods of electron diffraction microscopy of thin foils in transmission, indicates the presence of grains of the  $\alpha$  phase in the volume (solid solution based on iron, BCC crystal lattice) of the crystals of plate morphology, formed, obviously, owing to martensitic  $\gamma \rightarrow \alpha$  transformation. In the vol-

ume and on the boundaries of crystals of the  $\alpha$  phase, particles of the carbide phase are revealed (iron carbide, cementite). The crystals of the  $\alpha$  phase are fragmented, i.e., broken into weakly disordered volumes (Fig. 3). On the boundaries of fragments, also particles of the carbide phase are located.

Characteristic electron microscopic images of the structure of repeatedly applied cladding, are shown in Fig. 4. It is clearly seen that the formed material is multiphase. One of the phases is represented by inclusions of submicron sizes, poorly amenable to polishing (Fig. 4a, inclusions are shown by arrows). Following

**Table 2.** Phase composition and characteristics of the crystal structure of phases of single cladding

Phase	Parameters of phases				
	$\Delta V$ , wt %	$a$ , nm	$c$ , nm	$D$ (CSR), nm	$\Delta d/d$ , $10^{-3}$
$\alpha$ -Fe	63.2	0.28836		24.53	2.03
$\text{Fe}_3\text{O}_4$	28.8	0.28992	0.93832	9.85	7.254
$\text{Fe}_3\text{C}$	6.0	0.47146	0.44300	14.04	3.395
CrC	2.0	0.40610		10.55	2.914

$\Delta V$ —weight fraction;  $a$ ,  $b$ ,  $c$ —parameters of the elementary cell;  $D$  (CSR)—size of the regions of coherent scattering;  $\Delta d/d$ —microdistortions of the crystal lattice.

**Table 3.** Phase composition and characteristics of the crystal structure of phases of repeatedly welded layer

Phase	Parameters of phases					
	$\Delta V$ , wt %	$a$ , nm	$b$ , nm	$c$ , nm	$D$ (CSR), nm	$\Delta d/d$ , $10^{-3}$
$\text{M}_{23}\text{C}_6$	52.3	1.09122			21.93	9.102
$\alpha$ -Fe	46.7	0.28838			38.89	4.71
$\text{Nb}_6\text{C}_5$	1.0	0.54470	0.9435	0.5447		

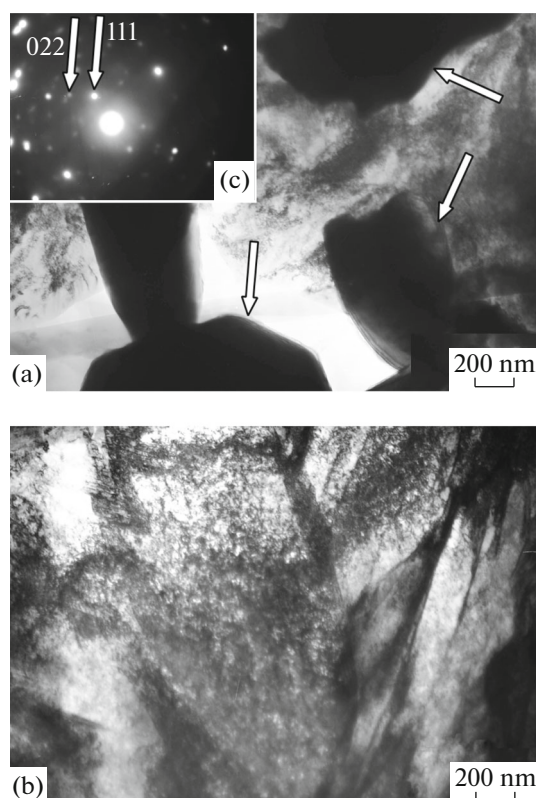


**Fig. 4.** Electron microscopic image of multiphase structure of repeated cladding on steel; in panel (c), indices of reflexes of niobium carbide NbC are indicated.

the results obtained by the methods of X-ray analysis (Table 3), one can conclude that these inclusions are the carbide phase, namely, carbides of the composition  $M_{23}C_6$  ( $(Cr, Fe, W)_{23}C_6$ ). The second phase is well polished and obviously is a solid solution based on  $\alpha$ -iron (bcc lattice) (Fig. 4b).

A characteristic electron microscopic image of the structure of the  $\alpha$  phase of repeated cladding is shown

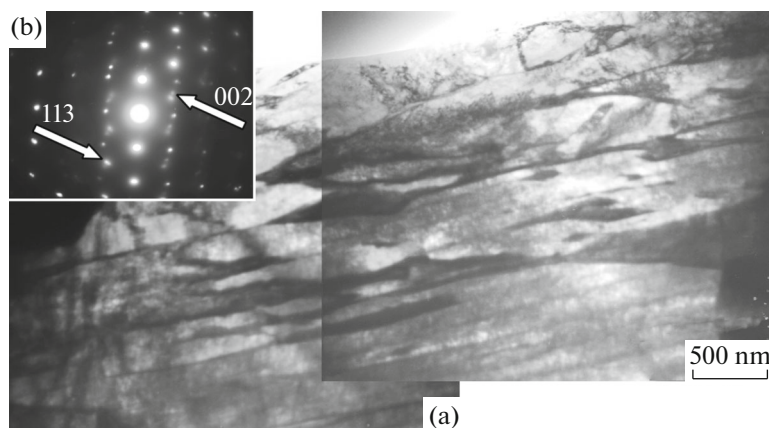


**Fig. 5.** Electron microscopic image of the structure of the  $\alpha$  phase of repeated cladding on steel (a); in panel (b), indices of reflexes of the  $\gamma$  phase are indicated.

in Fig. 5. The plate structure is clearly seen, formed by the martensitic mechanism of  $\gamma \rightarrow \alpha$  transformation. Indexing of micro electron diffraction patterns obtained with such a structure allowed revealing reflexes of the  $\alpha$  phase and  $\gamma$  phase (residual austenite, solid solution on the basis of fcc of the crystal lattice of iron) (Fig. 5b, reflexes of the  $\gamma$  phase are shown).

In the volume of martensite crystals, a dislocation substructure is found in the form of multidimensional grids (Fig. 4b); the scalar density of dislocations is greater than  $10^{11} \text{ cm}^{-2}$ . In some cases, in the volume of martensite crystals, transformation twins are found (Fig. 6).

In the volume and on the boundaries of martensite crystals, nanosized particles of the second phase are found (Fig. 7, particles are specified by arrows). Indexing of micro electron diffraction patterns obtained from such parts of the material showed that these particles are niobium carbide of the composition NbC.

In individual cases, it is possible to obtain micro electron diffraction patterns of the particles of submicron sizes. Indexing of such micro electron diffraction patterns made it possible to identify both reflexes of carbide  $M_{23}C_6$  ( $(Cr, Fe, W)_{23}C_6$ ), as well as reflexes of carbide NbC (Fig. 4c). Consequently, particles of submicron sizes in the cladding studied by us may be both niobium carbides and carbides of a more complex composition.

The structure of the metal contact area of the welding layer and base material is characteristic of tempered martensite—martensite crystals with relatively low scalar density of dislocations; in the volume and the crystal boundaries, particles of iron carbide are located.

## CONCLUSIONS

Studies of the phase composition, defect substructure, and mechanical and tribological properties of the

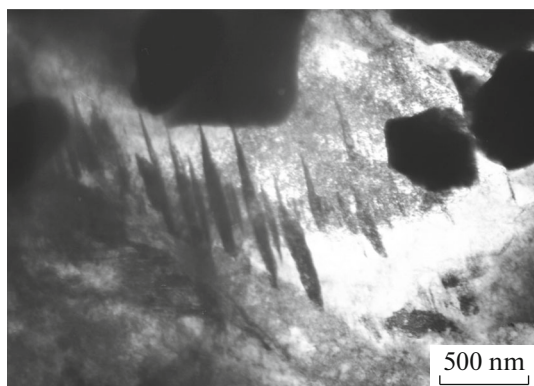


**Fig. 6.** Electron microscopic image of martensitic structure of repeated cladding on steel.

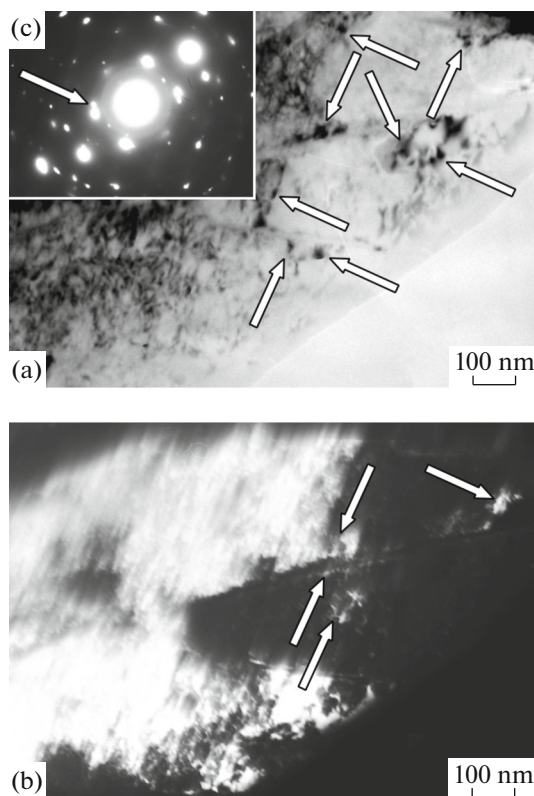


**Fig. 7.** Electron microscopic image of the structure of repeated cladding on steel; (a) light field; (b) dark field obtained in the reflex  $[110]\alpha\text{-Fe} + [002]\text{NbC}$  (reflexes are indicated in (c) by an arrow); (c) micro electron diffraction pattern to Fig. 7a. The arrows in (a) and (b) indicate particles of the carbide phase.

double cladding made on Hardox 450 steel by surfacing wire are performed. It is established that the wear resistance of the weld metal exceeds the wear resistance of Hardox 450 steel by 140–150 times; the fric-

tion coefficient of the weld metal is 2–2.5 times lower than the friction coefficient of steel.

It is shown that the formation of the second weld layer hardly affects the tribological characteristics of the material. It is established that increased mechanical and tribological properties of the weld layer are caused by the formation of multiphase submicro- and nanosized structure, hardening of which is associated with the formation of martensitic structure of  $\alpha$ -matrix and the presence of a high (over 50%) volume fraction of inclusions of carbide phase based on iron, chromium, tungsten, and niobium.

#### ACKNOWLEDGMENTS

This study was performed through a grant of the Russian Science Foundation (project no. 15-19-00065). In conducting the studies, equipment of the Center of Collective Use Material Engineering of Siberian State Industrial University was used.

#### REFERENCES

1. Poletika, I.M., Makarov, S.A., Tetyutskaya, M.V., and Krylova, T.A., Electron beam welding of wear- and corrosion-resistant coatings on mild steel, *Izv. Tomsk. Politekh. Univ.*, 2012, vol. 321, no. 2, pp. 86–89.
2. Sokolov, G.N. and Lysak, V.I., *Naplavka iznosostoikikh splavov na pressovye shampy dlya goryachego deformirovaniya stali* (Welding of Wear-Resistant Alloys on the Forged Stamps for the Hot Deformation of Steel), Volgograd: Politekhnik, 2005.
3. Kapralov, E.V., Budovskikh, E.A., Gromov, V.E., Raikov, S.V., and Ivanov, Yu.F., *Struktura i svoystva kompozitsionnykh iznosostoikikh naplavok na stal'* (The Structure and Properties of the Wear-Resistant Composite Welds on Steel), Novokuznetsk: Sib. Gos. Ind. Univ., 2014.
4. Kapralov, E.V., Budovskikh, E.A., Gromov, V.E., Raikov, S.V., Glezer, A.M., and Ivanov, Yu.F., The structure and properties of wear-resistant weld Hardox 400 on steel, *Probl. Chern. Metall. Materialoved.*, 2015, no. 1, pp. 80–86.
5. Kapralov, E.V., Budovskikh, E.A., Gromov, V.E., and Ivanov, Yu.F., Nanostructural states and properties of the surfacing formed on steel by a cored wire, *Russ. Phys. J.*, 2015, vol. 58, no. 4, pp. 471–477.
6. Grnezh, B., Use of Hardox steel in the mining industry, *Gorn. Prom.*, 2008, no. 3 (79), pp. 34–38.
7. Schastlivtsev, V.M., Mirzaev, D.A., and Yakovleva, I.L., *Struktura termicheskoi obrabotannoi stali* (The Structure of the Thermally Processed Steel), Moscow: Metallurgiya, 1994.
8. Bernshtein, M.L., Kaputkina, L.M., and Prokoshkin, S.D., *Otpusk stali* (Tempering of Steel), Moscow: Mosk. Inst. Stali Splavov, 1997.

*Translated by Sh. Galyaltdinov*